Available at www.sciencedirect.com

ScienceDirect

journal homepage: www.elsevier.com/locate/he

Modeling of fluidized bed membrane reactors for hydrogen production from steam methane reforming with Aspen Plus

Genyin Ye[a], *Donglai Xie*[a,*], *Weiyan Qiao*[a], *John R. Grace*[b], *C. Jim Lim*[b]

[a]*MOE Key Laboratory of Enhanced Heat Transfer and Energy Conservation, South China University of Technology, Guangzhou 510640, P.R. China*

[b]*Department of Chemical and Biological Engineering, The University of British Columbia, 2360 East Mall, Vancouver, Canada V6T 1Z3*

ARTICLE INFO

Article history:
Received 4 January 2009
Received in revised form
21 March 2009
Accepted 22 March 2009
Available online 23 April 2009

Keywords:
Fluidized bed membrane reactor
Model
Hydrogen production
Aspen Plus

ABSTRACT

Hydrogen production via steam methane reforming with *in situ* hydrogen separation in fluidized bed membrane reactors was simulated with Aspen Plus. The fluidized bed membrane reactor was divided into several successive steam methane sub-reformers and membrane sub-separators. The Gibbs minimum free energy sub-model in Aspen Plus was employed to simulate the steam methane reforming process in the sub-reformers. A FORTRAN sub-routine was integrated into Aspen Plus to simulate hydrogen permeation through membranes in the sub-separator based on Sieverts' law. Model predictions show satisfactory agreement with experimental data in the literature. The influences of reactor pressure, temperature, steam-to-carbon ratio, and permeate side hydrogen partial pressure on reactor performances were investigated with the model. Extracting hydrogen *in situ* is shown to shift the equilibrium of steam methane reactions forward, removing the thermodynamic bottleneck, and improving hydrogen yield while neutralizing, or even reversing, the adverse effect of pressure.

1. Introduction

Hydrogen is a major industrial commodity, used as an intermediate in a number of chemical and metallurgical processes, for example in the production of ammonia and methanol, upgrading of heavy hydrocarbons, iron ore reduction and food processing [1]. Widespread usage of hydrogen, if generated in an advantageous manner, could contribute to alleviation of growing concerns about the world's energy supply, security, air pollution, and greenhouse gas emissions.

Most of the world's hydrogen is generated at large petroleum and chemical plants by steam reforming of natural gas in parallel fixed bed reactors within huge top-fired or side-fired furnaces, coupled with pressure swing adsorption (PSA) for hydrogen purification [2]. These reformers have disadvantages such as large temperature gradients, low heat transfer coefficients, carbon formation on catalyst, and thermodynamic equilibrium limitations [3]. To overcome these shortcomings, various fluidized bed membrane reactors (FBMR) were proposed by Adris et al. [4], Xie et al. [5], Dehkordi and Memari [6] and Abashar et al. [7]. While the advantages of FBMR appear to be significant, offsetting disadvantages and challenges are recognized [2]. For example, pure hydrogen is produced at a lower pressure; attrition and entrainment of catalysts can occur given the hydrodynamic environment and vigorous particle motion; the perm-selective membrane must be capable of sustaining high fluxes and withstanding the erosive action of the bed. Several reactor models have been developed to simulate FBMR processes. Adris et al. [1] developed a two-phase bubbling bed model for steam methane

* *Corresponding author*. Tel./fax: +86 20 22236985.
E-mail address: dlxie@scut.edu.cn (D. Xie).

0360-3199/$ – see front matter © 2009 International Association for Hydrogen Energy. Published by Elsevier Ltd. All rights reserved.
doi:10.1016/j.ijhydene.2009.03.047

Nomenclature

C_{ep}	membrane permeation capacity (membrane surface area/thickness), km
E_p	activation energy for permeation, J mol^{-1}
F_{CH_4}	CH_4 feed rate, kmol h^{-1}
k	pre-exponential factor, mol km^{-1} h^{-1} Pa$^{-0.5}$
m	number of sub-separators used in the model, –
P	reactor pressure, MPa
P_{MH_2}	hydrogen partial pressures in the membrane permeate side, Pa
P_{RH_2}	hydrogen partial pressures in the reactor side, Pa
Q_{H_2}	hydrogen permeation rate, mol h^{-1}
R	gas constant, J mol^{-1} K^{-1}
SC	steam-to-carbon ratio, –
T	temperature, K

Greek letter

η	permeation effectiveness factor, –

reforming coupled with hydrogen diffusion through membranes. This model was later extended by Dogan et al. [8] and Roy [9] to autothermal steam reforming with oxygen addition. Rakib and Alhumaizi [10] developed a bubble assemblage model based on the model of Kato and Wen [11]. Chen and Elnashaie [12] developed a steady state one-dimensional plug flow reactor (PFR) model for a circulating FBMR. Grace et al. [13] developed a thermodynamic equilibrium model to investigate the effects of various process parameters on reactor performance. Sarvar-Amini et al. [14] modeled the steam methane reforming process using Aspen Plus based on a two-phase hydrodynamic model.

Modeling of membrane reactors presents interesting challenges because of the coupling of selective diffusion through the permeable surface with chemical reactions and mass transfer on the reactor side [13]. Predictions from previous models were in good agreement with experimental data. However, except for Sarvar-Amini et al. [14], all other models were solved by FORTRAN, Matlab or other computer programs, which are not easily accessible to design engineers in industry. Various process simulators, such as Aspen Plus and Hysys, are employed widely for industrial process simulations. A fluidized bed membrane reactor model based on such popular process simulators could facilitate the usage of such models, and help chemical engineers to design such reactors and to simulate alternative hydrogen production processes, including those featuring FBMR.

2. Model development

2.1. Primary assumptions

A fluidized bed membrane reactor for pure hydrogen production by steam methane reforming is shown schematically in Fig. 1. Preheated high-temperature (usually 500–800 °C) and high-pressure (usually 1–3 MPa) methane and steam are premixed and fed into the reactor where the following principal reforming reactions take place, closely approaching thermodynamic equilibrium:

$$CH_4 + H_2O \Leftrightarrow CO + 3H_2 \quad \Delta H^{\theta}_{298} = 206\ \text{kJ/mol} \tag{1}$$

$$CO + H_2O \Leftrightarrow CO_2 + H_2 \quad \Delta H^{\theta}_{298} = -41.2\ \text{kJ/mol} \tag{2}$$

$$CH_4 + 2H_2O \Leftrightarrow CO_2 + 4H_2 \quad \Delta H^{\theta}_{298} = 165\ \text{kJ/mol} \tag{3}$$

Hydrogen perm-selective membrane assemblies (made of palladium or its alloy) are installed inside the fluidized bed. Hydrogen in the product synthesis gases permeates through the membranes surfaces, shifting the equilibrium of reactions forward to increase the yield of hydrogen. The permeated hydrogen can be carried away by sweep gas or extracted by a vacuum pump to reduce the hydrogen partial pressure on the permeate side.

To simplify the simulation of steam methane reforming and hydrogen separation processes in the FBMR, the domain sketched by the dashed box in Fig. 1 is considered for model development. To represent the characteristics of fluidized bed reactors, the model assumes:

1. One-dimensional plug flow of reaction gases along the reactor, i.e. gas composition only varies in the vertical direction with negligible axial dispersion.
2. Uniform temperature within the fluidized bed.
3. Pressure gradients are ignored both within the reactor bed and within the membrane.

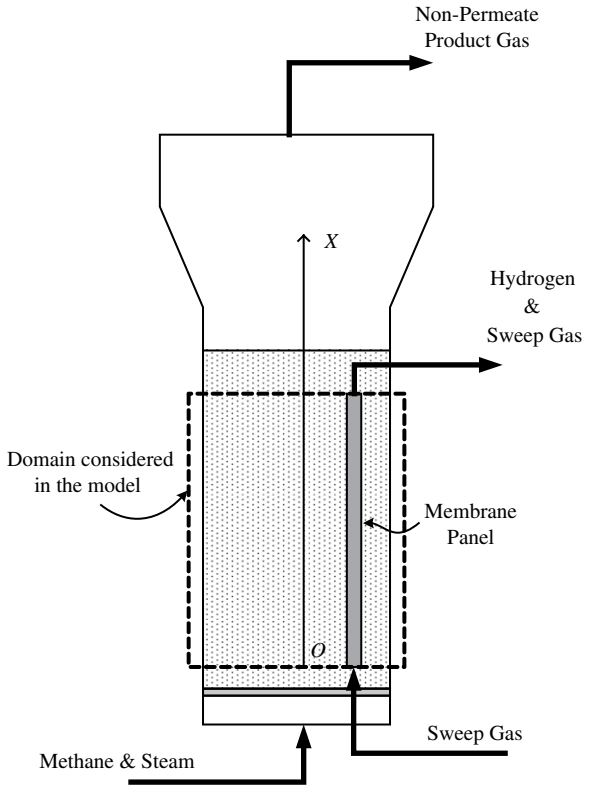

Fig. 1 – Schematic of a fluidized bed membrane reactor.

4. The steam methane reforming reactions reach thermodynamic equilibrium locally, i.e. the Gibbs free energy is assumed to reach a minimum locally.
5. Hydrogen permeation through the membrane follows Sieverts' law [15], i.e.

$$Q_{H_2} = \eta k C_{ep}\left[P_{RH_2}^{0.5} - P_{MH_2}^{0.5}\right] e^{\left(-\frac{E_p}{RT}\right)} \quad (4)$$

The co-existence of H_2O, CO, CO_2 or CH_4 has been reported to have a negative influence on the membrane separation performance [16]. This negative effect is considered in the permeation effectiveness factor – η, together with some other factors influencing the membrane performance, like the existence of a membrane substrate. In practice, η must be determined experimentally.

2.2. Simulation with Aspen Plus

Aspen Plus, one of the most important process simulators in the chemical industry and oil refining process, includes standard, ideal unit operations, such as Gibbs reaction and heat exchange models. Fluidized bed membrane reactor (FBMR) operation does not exist in the simulator. To simulate the FBMR process with Aspen Plus, a sequential modular approach was implemented. As illustrated in Fig. 2, the FBMR is divided into several successive steam methane sub-reformers and membrane sub-separators. As the steam methane reforming reactions reach thermodynamic equilibrium locally, the Gibbs reactor model in Aspen Plus is employed to simulate the synthesis gas production process in the sub-reformer. Free energy minimization is performed in the Gibbs reactor model to determine the product composition at which the Gibbs free energy of the products is a minimum. This course of action is useful when all the reactions occurring are unknown or are high in number due to many components participating in the reactions. As there is no separation model based on Sieverts' law [15] in Aspen Plus, a FORTRAN sub-routine was built and integrated into Aspen Plus to simulate hydrogen permeation through the membranes as described by Eq. (4). The input arguments of the sub-routine are η, k, C_{ep}, P_{RH_2}, P_{MH_2}, E, R, and T. This sub-routine calculates the hydrogen permeation rate Q_{H_2} as an output based on Eq. (4). The sub-routine program is listed in Appendix 1. After the user model (sub-routine) was built, it was compiled using the "aspcomp" procedure in Aspen Plus. Overall, the FBMR process is represented by $(m+1)$ sub-reformers and m sub-separators. Each sub-separator has a membrane permeation capacity of C_{ep}/m. The reactor off-gases from the ith sub-reformer are fed to the ith sub-separator, the non-permeated gases from the ith sub-separator are fed to the (i + 1)th sub-reformer, and the permeated hydrogen from the ith sub-separator accumulates in the (i + 1)th sub-separator. The feed to the FBMR constitutes the feed gases to the first sub-reformer.

Compared to the models of Adris et al. [1], Dogan et al. [8], Roy [9], Rakib and Alhumaizi [10] etc., the model of Sarvar-Amini et al. [14] and the present model are based on Aspen Plus. The latter provides a simple and quick method to simulate and optimize equilibrium-controlled processes such as hydrogen production. The model of Sarvar-Amini et al. [14] consists of hydrodynamic and reaction models, where the hydrodynamics are based on a two-phase model. The reformer is divided into two regions: a dense bed and freeboard. This model is complex and difficult to use compared to the current model.

2.3. Parameter determination

2.3.1. Species in the synthesis gas

Unlike kinetic models, reaction kinetics are not needed in Gibbs minimum free energy models. However, the product species must be specified. In this model, CH_4, H_2O, H_2, CO and CO_2 are considered to form the reactor off-gas. Other species, like solid carbon, could be easily added, but both experimental and theoretical studies show that carbon formation is not an issue in fluidized bed membrane reactors, so it is not considered in the current model.

2.3.2. Number of sub-separators

At $m = 0$, the model represents a regular Gibbs fluidized bed reactor without any hydrogen separation; $m = 1$ represents a case with only one separator and two sub-reformers, so that the hydrogen separation process is isolated from the synthesis gas production process. $m = 2$ represents a case with two sub-separators and three sub-reformers, wherein each sub-separator has a membrane permeation capacity of $C_{ep}/2$. The greater the number of sub-separators employed in the model, the more closely the sequential modular approach

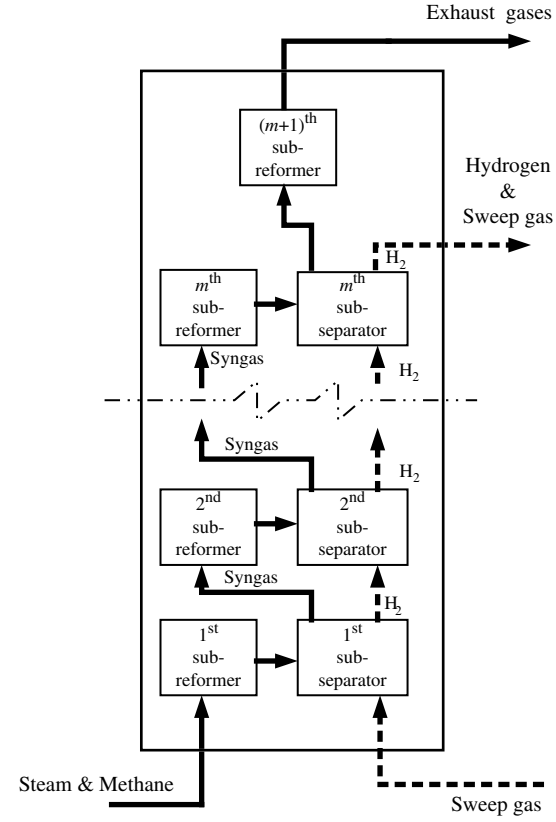

Fig. 2 – Sequential modular simulation diagram of FBMR with Aspen Plus.

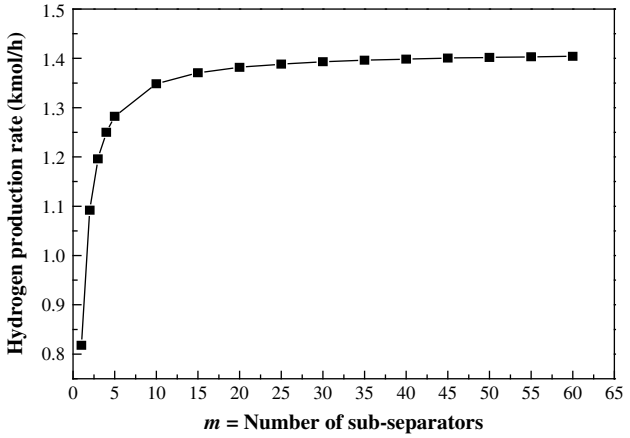

Fig. 3 – Influence of the number of sub-separators on the predicted hydrogen production rate. (F_{CH_4} = 1 kmol/h, P = 2 MPa, T = 600 °C, SC = 3, P_{MH_2} = 0.1 MPa, η = 1.)

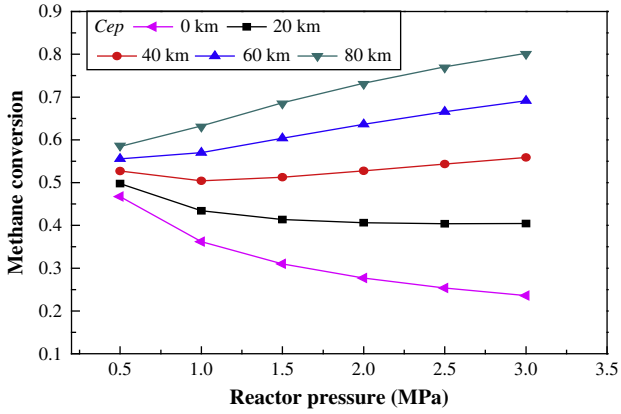

Fig. 4 – Influence of reactor pressure and membrane permeation capacity on methane conversion. (F_{CH_4} = 1 kmol/h, T = 600 °C, SC = 3, P_{MH_2} = 0.1 MPa, η = 1.)

method should represent the real FBMR process. In practice, m should be high enough to ensure that the predicted hydrogen production rate from the model is virtually independent of m. Fig. 3 shows the influence of m on the predicted hydrogen production rate for a typical case: methane feed $F_{CH_4} = 1\ \text{kmol h}^{-1}$, reactor pressure $P = 2$ MPa, reactor temperature $T = 600\ ^\circ$C, steam-to-carbon ratio SC = 3, pressure on membrane side $P_{MH_2} = 0.1$ MPa, membrane permeation capacity $C_{ep} = 40$ km. It can be seen that for $m > 50$, the influence of m on hydrogen yield is negligible. So m can be taken as 50 for the simulations. In the following simulations for various values of C_{ep}, a number of m values were selected, and it was proven in each case that its influence on the hydrogen production rate was negligible.

3. Comparison of model predictions with experimental data of Adris et al. [3]

Although the FBMR process was intensively studied by some researchers in recent years, very few experimental data are available from the literature for model validations. Experimental results from pilot-scale fluidized bed membrane reactor investigations were reported by Adris et al. [3] for reaction temperatures from 720 to 930 K and steam-to-carbon molar feed ratio (SC) of 2.4. The reactor has a diameter of 97 mm and length of 1.143 m. Twelve thin-walled (nominal wall thickness of 0.20–0.28 mm) palladium membrane tubes, each of outside diameter 4.7 mm were installed in the reactor. The Aspen Plus model is tested against the data obtained from these experiments. Table 1 compares the model predictions and experimental data for methane conversion (X_{CH_4}), hydrogen production rate from the membrane, and product gas composition. The permeation efficiency η is taken as 0.39, as suggested by Adris et al. [3]. The model predictions are seen to be in good agreement with the experimental data.

4. Parametric investigations

A parametric investigation can provide insights into the effects of major operating variables and design parameters on the performance of the reactor. In addition, the performance of the FBMR system can be explored beyond the range of

Table 1 – Comparison between equilibrium model predictions and experimental data of Adris et al. [3]. (F_{CH_4} = 74.2 mol/h, SC = 2.4, P = 0.98 MPa, C_{ep} = 0.4 km, sweep gas flow = 80 mol/h.)

Bed temperature (K)		720	767	815	867	913
Methane conversion X_{CH_4}	Experiment	0.12	0.18	0.264	0.366	0.479
	Predicted	0.11	0.16	0.221	0.335	0.42
Hydrogen production rate Q_{H_2} (mol h^{-1})	Experiment	1.7	2.5	3.57	4.81	6.23
	Predicted	1.77	2.55	3.61	4.95	6.30
		Product gas composition (vol%, dry basis)				
CH_4	Experiment	61.7	49.6	37.6	27.3	19.5
	Predicted	62.7	52.3	42.3	32.1	24.0
CO	Experiment	0.1	0.4	1.2	3.2	5.6
	Predicted	0.3	0.5	1.24	2.6	4.7
CO_2	Experiment	9.5	11.5	13	13.5	13.3
	Predicted	7.6	9.5	10.8	11.7	11.7
H_2	Experiment	28.7	38.5	48.2	56	61.6
	Predicted	29.4	37.6	45.9	55.3	59.5

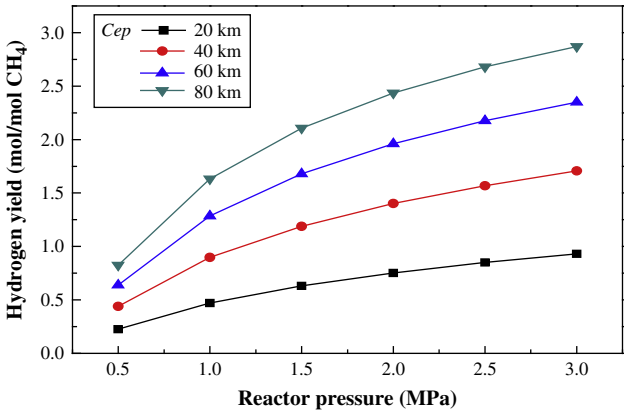

Fig. 5 – Influence of reactor pressure and membrane permeation capacity on hydrogen yield. (F_{CH_4} = 1 kmol/h, T = 600 °C, SC = 3, P_{MH_2} = 0.1 MPa, η = 1.)

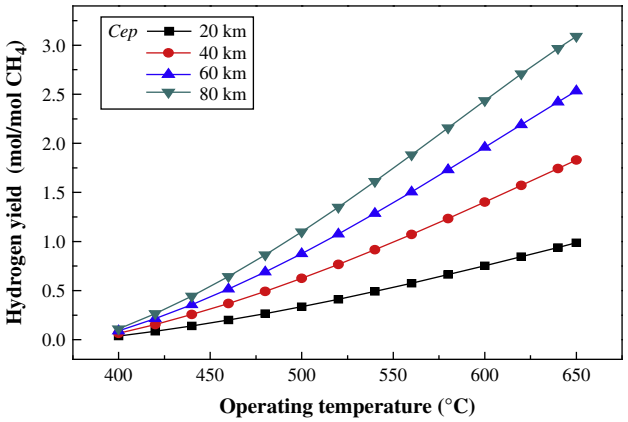

Fig. 7 – Influence of temperature and membrane permeation capacity on hydrogen yield. (F_{CH_4} = 1 mol/h, P = 2 MPa, SC = 3, P_{MH_2} = 0.1 MPa, η = 1.)

parameters that can be studied experimentally due to limitations imposed by economic and safety considerations. The performance of the FBMR is influenced by operating variables, like the reactor pressure, temperature, steam-to-carbon molar ratio, and permeate side hydrogen partial pressure. The influence of these factors on methane conversion and hydrogen yield, defined as the molar pure hydrogen production rate through the membranes per molar feed rate of methane, was predicted by the model.

4.1. *Influence of reactor pressure and membrane permeation capacity*

The thermodynamic equilibrium of steam reforming follows Le Chatelier's principle, so that conversions of reactions (1) and (3) benefit from low pressure, whereas reaction (2), the water-gas shift reaction, is independent of pressure. In an FBMR system, a perm-selective membrane installed in the fluidized bed reduces the adverse effect of high pressure by removing product moles, while also creating a higher driving force for permeation. Fig. 4 shows the influence of reaction pressure and membrane permeation capacity on methane conversion. At low permeation capacity (C_{ep} = 0, 20 km), methane conversion decreases with increasing reactor pressure, indicating that the reforming process dominates the FBMR process. At medium permeation capacity (C_{ep} = 40 km), the influence of pressure on methane conversion is almost neutral. If a very high permeation capacity (C_{ep} = 60, 80 km) could be used, methane conversion would increase with increasing reactor pressure, indicating that membrane permeation would dominate the FBMR process.

Fig. 5 shows the influence of reaction pressure and membrane permeation capacity on hydrogen yield. It can be seen that the hydrogen yield increases with increasing reactor pressure for all membrane permeation capacities tested. It can be seen from Figs. 4 and 5 that for C_{ep} = 20 km, methane conversion decreases with increasing reactor pressure. However, due to the increased driving force for hydrogen permeation through membranes at an elevated

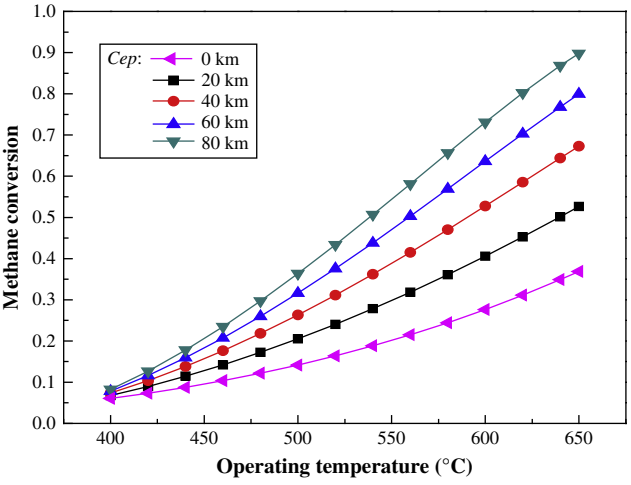

Fig. 6 – Influence of temperature and membrane permeation capacity on methane conversion. (F_{CH_4} = 1 kmol/h, P = 2 MPa, SC = 3, P_{MH_2} = 0.1 MPa, η = 1.)

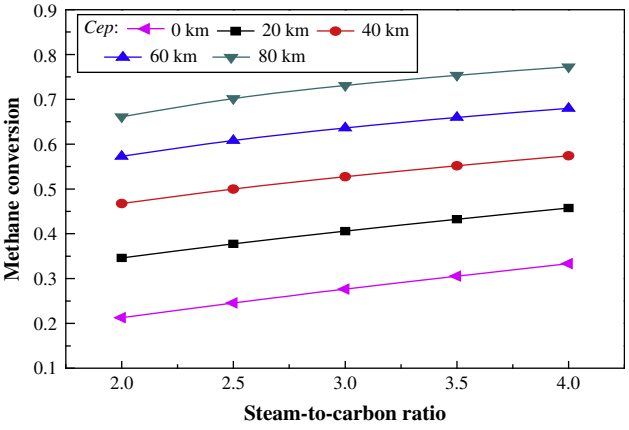

Fig. 8 – Influence of steam-to-carbon ratio and membrane permeation capacity on methane conversion. (F_{CH_4} = 1 kmol/h, P = 2 MPa, T = 600 °C, P_{MH_2} = 0.1 MPa, η = 1.)

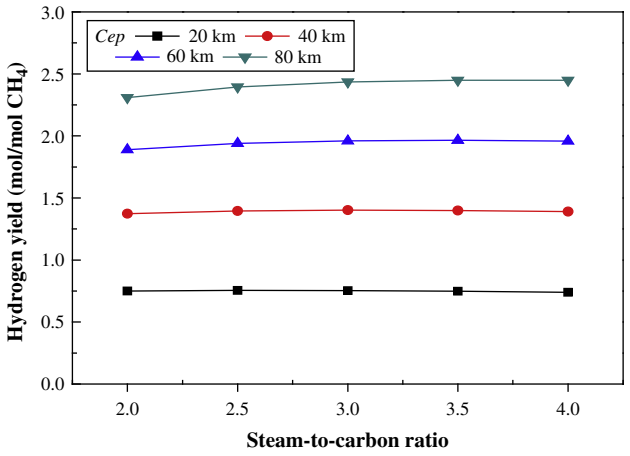

Fig. 9 – Influence of steam-to-carbon ratio and membrane permeation capacity on hydrogen yield. (F_{CH_4} = 1 kmol/h, P = 2 MPa, T = 600 °C, P_{MH_2} = 0.1 MPa, η = 1.)

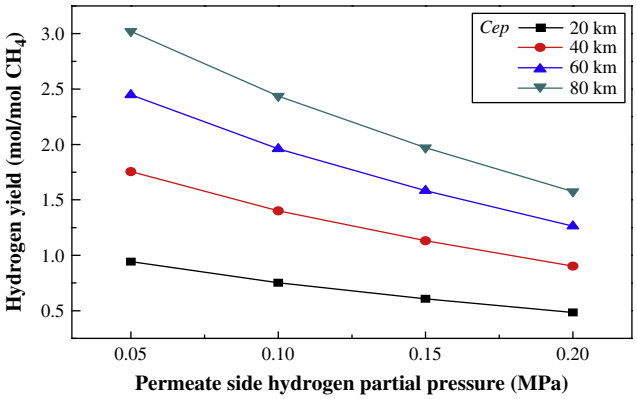

Fig. 11 – Influence of the permeate side pressure and membrane permeation capacity on hydrogen yield. (F_{CH_4} = 1 kmol/h, P = 2 MPa, T = 600 °C, SC = 3, η = 1.)

pressure, the hydrogen yield increases with increasing reactor pressure.

4.2. *Influence of temperature and membrane permeation capacity*

Both the methane conversion and hydrogen yield increase with increasing reactor temperature as shown in Figs. 6 and 7, respectively. The influence of temperature on methane conversion and hydrogen yield is more significant at higher membrane permeation capacities. It should be noted that the current membranes must not exceed ≈650 °C, so results are only plotted up to that temperature.

4.3. *Influence of steam-to-carbon ratio*

The lower limit of the steam-to-carbon ratio is governed by carbon formation and catalyst re-oxidation. Fig. 8 shows the predicted influence of the steam-to-carbon molar ratio on methane conversion. Methane conversion increases with increasing steam-to-carbon ratio. However, the hydrogen yield does not seem to be significantly influenced by the steam-to-carbon ratio, as illustrated in Fig. 9 for the range of conditions investigated. Based on the Le Chatelier's principle, a high steam-to-carbon ratio could increase the reaction conversion. However, a high steam feed rate would reduce the hydrogen partial pressure in the reactor, thereby diminishing the driving force for hydrogen permeation through membrane surfaces. These two counteracting effects approximately balanced each other for the conditions investigated, with the result that there was relatively little influence on the hydrogen yield.

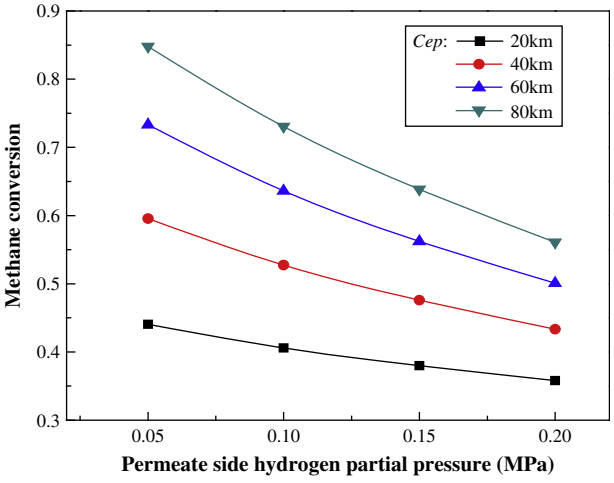

Fig. 10 – Influence of the permeate side pressure and membrane permeation capacity on methane conversion. (F_{CH_4} = 1 kmol/h, P = 2 MPa, T = 600 °C, SC = 3, η = 1.)

4.4. *Influence of permeate side hydrogen partial pressure*

A sweep gas such as steam can be employed to reduce the hydrogen partial pressure on the membrane side, thereby augmenting permeation. However, this would add a mass transfer resistance on the permeate side, and impurities in the water used to generate the steam would contaminate the hydrogen product. Vacuum is therefore likely to be employed to reduce the hydrogen pressure on the permeate side. Figs. 10 and 11 show the influence of the permeate side hydrogen partial pressure on methane conversion and hydrogen yield, respectively. Both methane conversion and hydrogen yield increase with decreasing hydrogen partial pressure on the permeate side. With higher C_{ep}, the predicted influence is more significant.

5. Conclusions

The hydrogen production process with steam methane reforming and *in situ* membrane separation technologies in fluidized bed membrane reactors is simulated with Aspen Plus. Model predictions on reactor performance show satisfactory agreement with experimental results in the literature. Parametric studies with the model show that for the FBMR:

1. Over the range of conditions investigated, at low permeation capacity, methane conversion decreases with increasing reactor pressure. At medium permeation capacity, the influence of pressure on methane conversion is almost neutral. At high permeation capacity, methane conversion increases with increasing reactor pressure.
2. For the conditions studied, hydrogen yield is improved by increasing reactor pressure for all membrane permeation capacities.
3. Both methane conversion and hydrogen yield increase with increasing operation temperature. The influence of reaction temperature on methane conversion and hydrogen yield is more significant with higher membrane permeation capacities.
4. Methane conversion increases with increasing steam-to-carbon ratio. However, the hydrogen yield is not significantly influenced by the steam-to-carbon ratio.
5. Methane conversion and hydrogen yield decrease with increasing hydrogen partial pressure on the permeate side. With higher C_{ep}, the influence is more significant.

Acknowledgment

Financial support from the National Natural Science Foundation of China (project # 20876054) is gratefully acknowledged.

Appendix 1
FORTRAN sub-routine program

```
#include ''dms_ncomp.cmn''

  C THIS SUBROUTINE WILL SPLIT AN INLET
    TO TWO OUTLETS
  C RETRIEVE THE SPLIT FACTOR
  C DECLARE ARGUMENTS
    INTEGER IDXSUB(NSUBS),ITYPE(NSUBS), INT(NINT),
    + IDS(2,13), NBOPST(6,NPO),
    + IWORK(NIWORK),INTSIZ(NSIZE),NSIN, NINFI,
    + NSOUT, NINFO, NREAL, LD, I
    REAL*8 SIN1(1), SIN2(1), SIN3(1),
    + SIN4(1), SOUT1(1), SOUT2(1),
    + SOUT3(1), SOUT4(1), WORK(NWORK),
    + SIZE(NSIZE), SINFI, SINFO
  C DECLARE LOCAL VARIABLES
    INTEGER IMISS
    REAL*8 REAL(NREAL), RMISS, SPLIT
  C BEGIN EXECUTABLE CODE
! INTEGER NCOMP_NCC
    REAL*8 K,E,R,T,pH,PL_H2,P,FRAC_H2,FRAC_H21
    REAL*8 OUT_DH2,DC,PL,C,H,A,B
    REAL*8 FIN_MOL(NCOMP_NCC+1)
    REAL*8 FIN_MOL1(NCOMP_NCC+1),
    REAL*8 PHEND,OUT_H2
    PARAMETER (K=1.084E-10,E=9.18E03,R=8.3145)
    T=SIN1(NCOMP_NCC+2) !Membrane Temperature
    P=SIN1(NCOMP_NCC+3) !H2 Partial pressure, high
    C=REAL(1); !membrane area
    H=REAL(2); !membrane foil thickness
    PL_H2=real(3); !Partial pressure of hydrogen, low
    OUT_DH2=0 !Initialition
    DC=C/10000
    DO 50 I = 1, NCOMP_NCC+1
    FIN_MOL(I) = SIN1(I)
 50 CONTINUE
    FRAC_H2=FIN_MOL(1)/FIN_MOL(NCOMP_NCC+1)
    pH=FRAC_H2*P
    IF(pH<PL_H2) THEN
     OUT_DH2=0
    ELSE
    DO I=1,10000
     OUT_H2=K*(pH**0.5-PL_H2**0.5)*EXP(-E/R/T)*DC/H
     OUT_DH2=OUT_DH2+OUT_H2
     FIN_MOL(1)=FIN_MOL(1)-OUT_H2
     FIN_MOL(NCOMP_NCC+1)=FIN_MOL(NCOMP_NCC+1)
     -OUT_H2
     pH=FIN_MOL(1)/FIN_MOL(NCOMP_NCC+1)*P
    end do
    END IF
    SOUT2(1)=SINT2(1)+OUT_DH2;
    SOUT2(2)=0;
    SOUT2(3)=0;
    SOUT2(4)=0
    SOUT2(5)=0
    SOUT2(6)=0
    SOUT2(7)=0
    SOUT2(NCOMP_NCC+1)=SUM(SOUT2);
    SOUT1(1) = SIN1(1)-SOUT2(1);
     DO 100 I=2,NCOMP_NCC+1
     SOUT1(I)=SIN1(I)
100 CONTINUE
    SOUT2(NCOMP_NCC+2) = SIN1(NCOMP_NCC+2)
    SOUT2(NCOMP_NCC+3) = SIN2(NCOMP_NCC+3)
     DO 200 I = NCOMP_NCCt2, NCOMP_NCC+3
     SOUT1(I) = SIN1(I)
200 CONTINUE
    RETURN
    END
```

REFERENCES

[1] Adris AM, Lim CJ, Grace JR. The fluidized-bed membrane reactor for steam methane reforming: model verification and parametric study. Chem Eng Sci 1997;52:1609–22.
[2] Grace JR, Elnashaie SSEH, Lim CJ. Hydrogen production in fluidized beds with in-situ membranes. Int J Chem Reactor Eng 2005;3:A41. Available at: <http://www.bepress.com/ijcre/vol3/A41>.
[3] Adris AM, Lim CJ, Grace JR. The fluidized bed membrane reactor system: a pilot scale experimental study. Chem Eng Sci 1994;49:5833–43.
[4] Adris AM, Elnashaie SSEH, Hughes R. Fluidized bed steam reforming of methane. Can J Chem Eng 1991;69:1061–70.
[5] Xie D, Lim CJ, Grace JR, Adris AM. Gas and particle circulation in an internally circulating fluidized bed membrane reactor cold model. Chem Eng Sci; in press, doi: 10.1016/j.ces.2009.02.032.

[6] Dehkordi AM, Memari M. Compartment model for steam reforming of methane in a membrane-assisted bubbling fluidized-bed reactor. Int J Hydrogen Energy 2009;34:1275–91.
[7] Abashar MEE, Alhabdan FM, Elnashaie SSEH. Discrete injection of oxygen enhances hydrogen production in circulating fast fluidized bed membrane reactors. Int J Hydrogen Energy 2008;63:2752–62.
[8] Dogan M, Posarac D, Grace JR, Adris AM, Lim CJ. Modeling of auto-thermal steam methane reforming in a fluidized bed membrane reactor. Int J Chem Reactor Eng 2003;1:1–12.
[9] Roy S. Fluidized bed steam reforming with high-flux membrane reforming: experimental verification and model validation. PhD thesis, University of Calgary, Alberta; 1998.
[10] Rakib MA, Alhumaizi KI. Modeling of a fluidized bed membrane reactor for the steam reforming of methane: advantages of oxygen addition for favorable hydrogen production. Energy Fuels 2005;19:2129–39.
[11] Kato K, Wen C. Bubble assemblage model for fluidized bed catalytic reactors. Chem Eng Sci 1969;24:1351–7.
[12] Chen Z, Elnashaie SSEH. Steady-state modeling and bifurcation behavior of circulating fluidized bed membrane reformer–regenerator for the production of hydrogen for fuel cells from heptane. Chem Eng Sci 2004; 59:3965–79.
[13] Grace JR, Li XT, Lim CJ. Equilibrium modeling of catalytic steam reforming of methane in membrane reactors with oxygen addition. Catal Today 2001;64:141–9.
[14] Sarvar-Amini A, Sotudeh-Gharehagh R, Bashiri H, Mostoufi N, Haghtalab A. Sequential simulation of a fluidized bed membrane reactor for the steam methane reforming using Aspen Plus. Energy Fuels 2007; 21:3593–8.
[15] Sieverts A, Zapf G. Solubility of H and D in solid Pd (I). Z Phys Chem 1935;A174:359–64.
[16] Unemoto A, Kaimai A, Sato K, Otake T, Yashiro K, Mizusaki J, et al. Surface reaction of hydrogen on a palladium alloy membrane under co-existence of H_2O, CO, CO_2 or CH_4. Int J Hydrogen Energy 2007;32:4023–9.